Title

Computer-Controlled CO2 Laser Ablation System for Cone-beam Computed Tomography and Digital Image Guided Endodontic Access: A Pilot Study

Journal

Journal of Endodontics, 47(9)

ISSN

0099-2399

Authors

Simon, Jacob C
Kwok, Jason W
Vinculado, Frank
et al.

Publication Date

2021-09-01

DOI

10.1016/j.joen.2021.06.004

Peer reviewed

HHS Public Access

Author manuscript

J Endod. Author manuscript; available in PMC 2022 February 24.

Published in final edited form as:

J Endod. 2021 September ; 47(9): 1445–1452. doi:10.1016/j.joen.2021.06.004.

Computer-Controlled CO_2 Laser Ablation System for Cone-beam Computed Tomography and Digital Image Guided Endodontic Access: A Pilot Study

Jacob C. Simon, DDS, PhD[*], **Jason W. Kwok, DDS**[†], **Frank Vinculado**[*], **Daniel Fried, PhD**[*]

[*]Department of Preventive and Restorative Dental Sciences, University of California San Francisco, San Francisco, California

[†]Department of Endodontology, University of Connecticut, Farmington, Connecticut

Abstract

Introduction: Ideal endodontic access provides unobstructed entry to the pulp chamber and visualization of the canal orifices while preserving the maximum amount of tooth structure. The aim of this study was to implement the use of lasers to accurately and predictably access teeth to follow the principles of minimally invasive endodontics.

Methods: Traditional, conservative, ultraconservative, bridge, truss, and orifice-directed accesses were performed. A computer-controlled 9.3-μm CO_2 laser ablation system was assembled and coupled with custom software capable of combining cone-beam computed tomographic (CBCT) volumetric data with spatially calibrated digital images of teeth to provide an augmented reality environment for designing and preparing endodontic accesses. Twenty ($N = 20$) sound posterior teeth with fully developed root canal systems were imaged with CBCT scans and accessed via laser ablation *in vitro*.

Results: All 20 (20/20) teeth were successfully accessed without iatrogenic errors. Volumetric renderings from post-access CBCT scans were used to verify the access and determine accuracy qualitatively. The volumetric measurements of hard tissue removed were as follows: traditional = 39.41 mm^3, conservative = 9.76 mm^3, ultraconservative = 7.1 mm^3, bridge = 11.53 mm^3, truss = 19.21 mm^3, and orifice directed = 16.86 mm^3.

Conclusions: Digital image guidance based on feature recognition and registration with CBCT data is a viable method to address the challenge of dynamic navigation for accessing the pulp chamber. Modern lasers with high pulse repetition rates integrated with computer-controlled scanning systems are suitable for the efficient cutting of dental hard tissues.

Keywords

Automated; dynamic navigation system; guided; endodontic access; laser

Address requests for reprints to Jacob C. Simon, Department of Preventive and Restorative Dental Sciences, University of California San Francisco, 707 Parnassus Avenue, San Francisco, CA 94142. jacob.simon@ucsf.edu 0099-2399.

Ideal endodontic access provides unobstructed opening to the pulp chamber and visualization of the canal orifices while preserving the maximum amount of tooth structure[1,2]. The practice of minimally invasive endodontics is important to preserve coronal and pericervical tooth structure[3]. The retention of coronal and pericervical hard tissue distributes coronal stress over a larger volume of natural tooth structure, therefore minimizing stress concentration and predisposition to coronal and root fracture[4–8]. It is generally well understood that the cumulative loss of tooth structure leads to the overall detriment of the tooth and reduced resistance to fracture[9–15]. In order to minimize the cumulative loss of tooth structure, it would be beneficial to implement a system that can accurately and predictably access teeth in a minimally invasive manner. Computer-aided dynamic navigation systems (DNSs) have been adapted from guided implant systems to address this need[16–22]. DNS technologies use thermoplastic molds with radiopaque fiducial markers to register cone-beam computed tomographic (CBCT) scans with tooth anatomy.

In this study, we present an alternative method to perform a minimally invasive access by using a computer-controlled, 9.3-μm CO_2 laser ablation system to access teeth based on spatially calibrated digital image guidance and CBCT scans. The samples in this pilot study were chosen at random from a pool of posterior teeth with fully developed roots and closed apices and then were screened with periapical radiographs to ensure mature pulpal anatomy. Distinct, invariant tooth anatomy is extracted from volumetric data from CBCT scans and then overlayed and registered with digital images of the tooth crown. An interactive augmented reality user interface computer generates the precise location of the internal anatomy and displays it through graphic projections in the digital image. A toolbox of drawing mechanisms is used by the clinician to design the access of choice through the software. In cases in which CBCT scans are unavailable, the clinician can design access using only the digital image, just as a clinician does with his or her eyes and hands currently. The access design is transformed into an algorithm that scans the CO_2 laser over the tooth, cutting the desired shape in a stepwise routine.

MATERIALS AND METHODS

Sample Preparation

Twenty ($N = 20$) posterior teeth with developed roots and closed apices were screened with periapical radiographs to ensure mature pulpal anatomy from a pool of extracted teeth collected from patients in the San Francisco Bay Area with approval from the University of California San Francisco Committee on Human Research. Using the American Association of Endodontists endodontic case difficulty assessment form and guidelines, samples qualifying as minimal and moderate difficulty for radiographic appearance of canal(s) criteria were included for participation in this study. A sample size of 20 teeth was chosen as a significant number of samples to demonstrate a variety of access designs in molar and premolar teeth. Samples were sterilized using gamma radiation by the University of California San Francisco central sterilization facility and stored in 0.1% thymol solution to maintain tissue hydration and prevent bacterial growth. Teeth were mounted in orthodontic resin blocks extending from the cementoenamel junction to 3–5 mm beyond the apices, leaving the crown exposed for ease of mounting in the sample holder.

In this study, different access designs are demonstrated and defined as follows: traditional (T), straight-line access; conservative (C), a contracted traditional access; ultraconservative (U), a centralized circular access of a 2-mm diameter or less; truss (Tr), a mandibular molar access design with separate mesial and distal preparations leaving a full-thickness connection of enamel and dentin between the buccal and lingual walls; bridge (B), a truss design with only a dentin connection between the buccal and lingual wall[12,23,24]; and orifice directed (O), circular or ovoid preparations less than a 2-mm diameter positioned directly coronal to the location of the canal orifices at the level of the pulpal floor.

CO_2 Laser Parameters

A Diamond J5-V CO_2 laser (Coherent, Santa Clara, CA) was integrated with a 3-dimensional computer-controlled ablation system[25]. The J5-V in this study produced a Gaussian output beam and operated at $\lambda = 9.3$ μm with a pulse duration of 26 microseconds and a pulse repetition rate of 100 Hz when cutting dentin or 200 Hz when cutting enamel. The laser energy output was monitored using a power/energy meter (ED-200; Gentec, Quebec, Canada), the beam profile was imaged using a Pyrocam Beam profilometer (Ophir-Spiricon, Logan, UT), and the laser pulse temporal profile was measured with a room temperature HgCdTe detector (PF-10.6-3; Boston Electronics, Boston, MA) with a response time of a few nanoseconds. The laser beam was focused with a (f = 100 mm) ZnSe scanning lens to a waist diameter of 200 μm measured by scanning a razor blade across the beam to determine the diameter ($1/e^2$). The incident fluence was 30 J/cm^2 and removed ~30 μm sound tissue structure per pulse confirmed through cross-polarized optical coherence tomographic scans (Model IVS-300-CP; Santec Corp, Komaki, Aichi, Japan) of ablated calibration samples.

Digital Images

Digital images were acquired with a digital microscope (Model AM2111; AnMO Electronics Corp, New Taipei City, Taiwan), and the 640 × 480 pixel array was calibrated with a lens distortion correctional algorithm in LabView Vision Assistant (National Instruments, Austin, TX) yielding an (x, y) accuracy of 23.7 μm/pixel. Fiducial points ablated into the occlusal surface of each sample were used to modify the calibration matrix from relative positional measurements to real-world coordinates.

CBCT Imaging

A CBCT scan was acquired of each sample using the K9000 CBCT unit (Kodak/Carestream, Rochester, NY) operating at 60 kV, 2.0 mA, a 24-second scan duration, and 33.1 mGy.cm^2 with 76.5-μm pixel spacing and 76.5-μm slice thickness over a limited field of view (5 cm × 7 cm). Scans were acquired before treatment, after laser access, and after crown-down filing.

Ablation System

The PXIe-8840 embedded controller (National Instruments, Austin, TX) and PXI-6259 data-acquisition module (National Instruments) in the PXIe-1062Q chassis (National Instruments) served as the computer control hardware for the subcomponents of the ablation system. Custom software was authored in LabView that integrated spatially calibrated

digital images and CBCT Digital Imaging and Communications in Medicine (DICOM) data; provided an augmented reality user interface for access design; produced ablation algorithms; and coordinated the laser output with x, y, z motion control stages VP-25XL and UTM50PPIHL from Newport (Irvine, CA) to cut guided endodontic accesses into the samples.

CBCT DICOM data are loaded into the LabView software and viewed as conventional axial, sagittal, and coronal orthoslices for treatment planning. The program was authored to permit 3-dimensional rotational correction of the slices in order to match the volumetric data to the true sample position in the digital image. The operator is permitted to angle the access design in 1 dimension, and the real-world cutting axis of the sample is adjusted to accommodate using a single-axis goniometer stage from ThorLabs (Newton, NJ). Using 3-dimensional image processing algorithms[26], subregions are manually selected and transformed into 2-dimensional compressed axial slices representing the cusp locations, height of contour, pulp chamber perimeter, and orifice location and shape. Additionally, a surface topographic rendering is produced. The CBCT extracts can be modified by manual selection using the “magic wand” feature, allowing control over exact contours and features to be used for registration verification and access design. The selected features are converted into region of interest variables and overlaid with the digital image of the sample to verify the height of contour and cusp locations confirming registration. Outlines of the pulp chamber and orifices then represent their true anatomic location relative to the current vantage point, and a suite of drawing tools and preprogrammed shapes are used to design the final access shape. Confirmation of the final design produces 2 scanning patterns; the first uses the topographic rendering to first guide the laser to reduce the slope of cusps, and the second scans the entire preparation area in a raster.

Samples are mounted in the laser path, and the program cuts the designed access using the 3 single-axis motorized stages. The first scanning pattern for cusp slope reduction is performed at 200 Hz, and the second for dentin preparation is performed at 100 Hz. All ablation is performed with water coolant, air spray, and a passive vacuum for the removal of debris accumulation.

Sample access was planned and executed in 1 sequence without modification in order to demonstrate the simple effectiveness of the CO_2 laser for accurate ablation.

Endodontic Treatment

After the access was executed, pulp chambers were irrigated with 4% hypochlorite and a #10 K-file, and an endodontic explorer was used to confirm canal presence and coronal patency. After CBCT imaging of the laser-produced access, a true crown-down preparation was performed to approximately two thirds of the root length using .10 and .08 taper K3 files. Canals were then prepared up to a #40/.06 Vortex Blue (Dentsply Sirona, Charlotte, NC) rotary file to approximately two thirds the canal length to demonstrate feasibility in treating the canal systems with all aforementioned accesses.

CBCT Image Analysis

DICOM files were analyzed using 3D Slicer, an open source software package for scientific visualization[27]. Pre- and post-laser and post–crown-down CBCT scans were segmented and 3-dimensionally rendered for visual/qualitative comparison. Volumetric data were measured for segmented sections to determine the amount of hard tissue removed in the preparations.

RESULTS

A variety of endodontic access cavities were successfully cut into 20 samples using a CO_2 laser ablation system without any iatrogenic misalignment, gouging, or perforation. Representative samples from the population demonstrating a range of designs are shown in Figure 1. Traditional (T), conservative (C), ultraconservative (U), bridge (B) or truss (Tr), and orifice-directed (O) accesses are presented with visible images 1–3 showing preablation, post–laser access, and post–crown-down treatments accompanied with volumetric renderings 4 and 5 showing the mesiodistal and buccolingual shape and angles. The volume of hard tissue removed from each sample was as follows: traditional (T) = 39.41 mm^3, conservative (C) = 9.76 mm^3, ultraconservative (U) = 7.1 mm^3, bridge (B) = 11.53 mm^3, and orifice directed (O) = 16.86 mm^3.

Figure 2 shows the results from the access of a mandibular molar prepared with a truss design centered over the mesial and distal radicular systems of before ablation (Fig. 2A), after laser access (Fig. 2B), and after the crown-down procedure (Fig. 2C). Volumetric renderings (Fig. 2D and E) are presented showing the positioning of preparations (*yellow*) in relation to orifice location (*red*) from the occlusal viewpoint after cutting with the CO_2 laser (Fig. 2D) and after the crown-down procedure (Fig. 2E). Volumetric renderings (Fig. 2F and G) illustrate the mesiodistal and buccolingual shape and angles. The truss access in this sample has a volume of 19.21 mm^3 hard tissue removed.

Two maxillary molars are presented in Figure 3 prepared with a conservative preparation (C) and an orifice-directed access (O). Figure 3C1–C3 and 3O1–O3 are preablation, post–laser access, and post–crown-down treatment. Figure 3C4 and C5 and 3*O4* and O5 show the positioning of preparations (*yellow*) in relation to orifice location (*red*) from the occlusal viewpoint after cutting with the CO_2 laser (Fig. 3C4) and after crown-down treatment (Fig. 3C5). Figure 3O4 and O5 are post–crown-down renderings illustrating clear visualization of the buccal (Fig. 3O4) and palatal (Fig. 3O5) systems. Figure 3C6 and C7 and 3O6 and O7 demonstrate the mesiodistal and buccolingual shape and angles. The maxillary accesses presented have a volume of C = 24.46 mm^3 and O = 19.65 mm^3 hard tissue removed.

DISCUSSION

The potential of a laser-based approach for selective caries removal and endodontic access preparation deserves renewed attention because of the improved performance and characteristics of newly developed infrared lasers compared with those researched over 20 years ago[28]. Carious and sound hard tissues can be selectively ablated in precise stepwise increments of ~30-μm depths. Ejected infected tissue and toxins are heated to high temperatures, reducing the contamination of more apical layers of hard or soft tissue[29].

When integrated with computer-controlled systems, laser pulses can be focused and directed with precision and accuracy to produce preparations at or smaller than the fundamen6tal limit of what is treatable with the current endodontic armamentarium.

The results demonstrated in this study show that a computer-controlled 9.3-μm CO_2 laser system can prepare a variety of endodontic access designs and can act as a dynamic navigation system by integrating CBCT volumetric data to produce an augmented reality environment permitting orifice-directed access. Unlike other dynamic navigation systems used in endodontics such as X-NAV (X-Nav Technologies, Lansdale, PA), this system can also operate without CBCT data due to the fact that this DNS integrates a digital image of the tooth into the computer interface. The clinician can digitally design the access based solely on the image of the occlusal surface, and the preparation is automatically performed by the computer-controlled laser. Therefore, emergency treatment or cases in which CBCT is unavailable can still be automatically performed and guided by the clinician.

In this pilot study, all of the access designs were preplanned using CBCT data and executed in 1 sequence without modification in order to demonstrate the simple effectiveness of the CO_2 laser for accurate ablation. Each scan of the laser ablates ~30 μm hard tissue, and a simple division of the desired cutting depth measured from the CBCT data by the ablation depth per scan was predetermined to automatically cut to and stop at the desired depth. There are other possible methods to control access depth when the true necessary depth is unknown. One exciting method is spectral feedback, which would be useful in teeth with existing pulp tissue. This method analyzes component wavelengths of the ablation plume to discriminate between hard and soft tissue by measuring the presence of calcium from its strong spectral emission peak at 605 nm[30,31]. A system based on this method could scan the laser without predetermining the depth and be programmed to automatically stop when the soft tissue of the pulp chamber has been reached. In a previous *in vivo* study, we demonstrated a CO_2 laser system that automatically ablated composites from teeth using spectral feedback[30]. That study delivered laser light through an articulating arm and bite block onto the occlusal tooth surface. That same mechanism can be adapted to be secured to the rubber dam clamp with 3-dimensional printing.

Another method to control the access depth would be to use a coaxial imaging and ablation design analogous to one we constructed for a study we performed demonstrating short-wave infrared imaging–guided caries ablation using a low-cost 9.3-μm laser (DL-500; Access Laser, Everett, WA)[32]. In this method, the CO_2 laser system can be scanned to a conservative set depth (ie, ablate 1 mm at a time), imaged with the coaxial beam and then presented to the clinician to verify the preparation location and shape, permitting alterations to the original design if necessary. The DL-500 CO_2 laser we used has similar characteristics to the one used here and would be suitable for a clinical system. Currently, both CO_2 and erbium lasers have Food and Drug Administration clearance for soft and hard tissue treatment.

A clinical computer-controlled laser system is ideally suited for image-guided or spectral-guided caries removal followed by endodontic therapy. Because of the fact that lasers operate in a sterile field, eject tissue, and provide hemostasis, pulpotomy procedures have the potential for a better prognosis. In particular, pediatric endodontics may find these

systems especially useful because of patient pain tolerance and the higher success rate of pulpotomy procedures of immature teeth[33–37]. When a complete root canal is planned, a computer-controlled laser system has the potential to reduce off-target and off-axis access preparations. CBCT-guided lasers may also be useful for accessing calcified canals by drilling very small and accurate orifices on a guided path. In preliminary attempts in simulated calcified incisors, we have been able to reach depths between 8–12 mm apical to the pulpal floor. We plan to investigate this further in future research studies. Lastly, if erbium lasers can ablate tissue at a clinically satisfactory standard relative to the CO_2 tested here, then clinicians who used the system could then employ the same laser for laser-activated irrigation.

The limitations of the laser ablation system as constructed is the reliance on x, y, z motion stages that limits the laser scanning rate. Scanning the laser over a 2-mm diameter circle takes 30 seconds, yielding a preparation time of 6 minutes to prepare a 2-mm diameter × 4-mm deep preparation. More complex access designs in this study took approximately 20 minutes to execute. Another limitation is that only tapered cylinder access shapes could be achieved because of the fact that the laser beam is stationary, and the sample is scanned in this *in vitro* setup. Avoiding excessive heat accumulation in the tooth will be the limiting variable for preparation speed in such systems. Figure 1T1–T5 demonstrates charred dentin at the perimeter of the access due to overheating. Excessive heat accumulation during laser irradiation can cause crack formation and the charring of dentin. Several studies have explored the laser parameters that cause peripheral thermal damage with pulsed CO_2 lasers[38–40]. Both limitations in preparation shape and heat distribution can be overcome by using a high-speed galvanometer, voice coil, or microelectromechanical scanning systems. Such scanning systems will also enable the use of angled incident laser beams allowing multiaxis angled beam delivery that will enable the cutting of inverted cones and hourglass-shaped access forms.

ACKNOWLEDGMENTS

The authors would like to acknowledge the support of NIDCR/NIH grants R01-DE019631 and F30-DE026052.

REFERENCES

1. Krapez J, Fidler A. Location and dimensions of access cavity in permanent incisors, canines, and premolars. J Conserv Dent 2013;16:404–7. [PubMed: 24082567]
2. Patel S, Rhodes J. A practical guide to endodontic access cavity preparation in molar teeth. Br Dent J 2007;203:133–40. [PubMed: 17694021]
3. Lin CY, Lin D, He WH. Impacts of 3 different endodontic access cavity designs on dentin removal and point of entry in 3-dimensional digital models. J Endod 2020;46:524–30. [PubMed: 32115250]
4. Yuan K, Niu C, Xie Q, et al. Comparative evaluation of the impact of minimally invasive preparation vs. conventional straight-line preparation on tooth biomechanics: a finite element analysis. Eur J Oral Sci 2016;124:591–6. [PubMed: 27704709]
5. Rover G, Belladonna FG, Bortoluzzi EA, et al. Influence of access cavity design on root canal detection, instrumentation efficacy, and fracture resistance assessed in maxillary molars. J Endod 2017;43:1657–62. [PubMed: 28739013]
6. Krishan R, Paque F, Ossareh A, et al. Impacts of conservative endodontic cavity on root canal instrumentation efficacy and resistance to fracture assessed in incisors, premolars, and molars. J Endod 2014;40:1160–6. [PubMed: 25069925]

7. Zhang Y, Liu Y, She Y, et al. The effect of endodontic access cavities on fracture resistance of first maxillary molar using the extended finite element method. J Endod 2019;45:316–21. [PubMed: 30803539]
8. Jiang Q, Huang Y, Tu X, et al. Biomechanical properties of first maxillary molars with different endodontic cavities: a finite element analysis. J Endod 2018;44:1283–8. [PubMed: 29910031]
9. Hussain SK, McDonald A, Moles DR. *In vitro* study investigating the mass of tooth structure removed following endodontic and restorative procedures. J Prosthet Dent 2007;98:260–9. [PubMed: 17936125]
10. Sedgley CM, Messer HH. Are endodontically treated teeth more brittle? J Endod 1992;18: 332–5. [PubMed: 1402595]
11. Plotino G, Grande NM, Isufi A, et al. Fracture strength of endodontically treated teeth with different access cavity designs. J Endod 2017;43:995–1000. [PubMed: 28416305]
12. Corsentino G, Pedulla E, Castelli L, et al. Influence of access cavity preparation and remaining tooth substance on fracture strength of endodontically treated teeth. J Endod 2018;44:1416–21. [PubMed: 30049468]
13. Wang Q, Liu Y, Wang Z, et al. Effect of access cavities and canal enlargement on biomechanics of endodontically treated teeth: a finite element analysis. J Endod 2020;46:1501–7. [PubMed: 32615176]
14. Saber SM, Hayaty DM, Nawar NN, Kim HC. The effect of access cavity designs and sizes of root canal preparations on the biomechanical behavior of an endodontically treated mandibular first molar: a finite element analysis. J Endod 2020 Jul 5. 10.1016/j.joen.2020.06.040 [Epub ahead of print].
15. Zelic K, Vukicevic A, Jovicic G, et al. Mechanical weakening of devitalized teeth: three-dimensional finite element analysis and prediction of tooth fracture. Int Endod J 2015;48:850–63. [PubMed: 25243348]
16. Zubizarreta-Macho A, Munoz AP, Deglow ER, et al. Accuracy of computer-aided dynamic navigation compared to computer-aided static procedure for endodontic access cavities: an *in vitro* study. J Clin Med 2020;9:129.
17. Mediavilla Guzman A, Riad Deglow E, Zubizarreta-Macho A, et al. Accuracy of computer-aided dynamic navigation compared to computer-aided static navigation for dental implant placement: an *in vitro* study. J Clin Med 2019;8:2123.
18. Chong BS, Dhesi M, Makdissi J. Computer-aided dynamic navigation: a novel method for guided endodontics. Quintessence Int 2019;50:196–202. [PubMed: 30773571]
19. Connert T, Zehnder MS, Weiger R, et al. Microguided endodontics: accuracy of a miniaturized technique for apically extended access cavity preparation in anterior teeth. J Endod 2017;43:787–90. [PubMed: 28292595]
20. Krastl G, Zehnder MS, Connert T, et al. Guided endodontics: a novel treatment approach for teeth with pulp canal calcification and apical pathology. Dent Traumatol 2016;32:240–6. [PubMed: 26449290]
21. Connert T, Zehnder MS, Amato M, et al. Microguided endodontics: a method to achieve minimally invasive access cavity preparation and root canal location in mandibular incisors using a novel computer-guided technique. Int Endod J 2018;51:247–55. [PubMed: 28665514]
22. Zehnder MS, Connert T, Weiger R, et al. Guided endodontics: accuracy of a novel method for guided access cavity preparation and root canal location. Int Endod J 2016;49:966–72. [PubMed: 26353942]
23. Abou-Elnaga MY, Alkhawas MA, Kim HC, Refai AS. Effect of truss access and artificial truss restoration on the fracture resistance of endodontically treated mandibular first molars. J Endod 2019;45:813–7. [PubMed: 30905571]
24. Silva E, Pinto KP, Ferreira CM, et al. Current status on minimal access cavity preparations: a critical analysis and a proposal for a universal nomenclature. Int Endod J 2020;53:1618–35. [PubMed: 32854167]
25. Ngo A, Chan KH, Simon JC, Fried D. Image-guided removal of interproximal lesions with a CO2 laser. Proc SPIE Int Soc Opt Eng 2018;10473:104730T.

26. Chan KH, Chan AC, Fried WA, et al. Use of 2D images of depth and integrated reflectivity to represent the severity of demineralization in cross-polarization optical coherence tomography. J Biophotonics 2015;8:36–45. [PubMed: 24307350]
27. Kikinis R, Pieper SD, Vosburgh KG. 3D Slicer: A Platform for Subject-Specific Image Analysis, Visualization, and Clinical Support. New York: Springer; 2014. p. 277–89.
28. Olivi G, De Moor R, DiVito E. Lasers in Endodontics: Scientific Background and Clinical Applications. New York: Springer International Publishing; 2016.
29. Hibst R, Stock K, Gall R, Keller U. Controlled tooth surface heating and sterilization by Er:YAG laser radiation. Proc SPIE 1996;2922:119–61.
30. Simon JC, Choi JH, Jang A, Fried D. *In vivo* spectral guided removal of composite from tooth surfaces with a CO2 laser. Proc SPIE Int Soc Opt Eng 2020;11217:112170K.
31. Yi I, Chan KH, Tsuji GH, et al. Selective removal of esthetic composite restorations with spectral guided laser ablation. Proc SPIE Int Soc Opt Eng 2016;9692:96920U.
32. Chan KH, Fried D. Selective ablation of dental caries using coaxial CO2 (9.3-μm) and near-IR (1880-nm) lasers. Lasers Surg Med 2019;51:176–84. [PubMed: 30024032]
33. Nazemisalman B, Farsadeghi M, Sokhansanj M. Types of lasers and their applications in pediatric dentistry. J Lasers Med Sci 2015;6:96–101. [PubMed: 26464775]
34. Zhang S, Chen T, Ge LH. [Evaluation of clinical outcomes for Er:YAG laser application in caries therapy of children]. Beijing Da Xue Xue Bao Yi Xue Ban 2013;45:87–91. [PubMed: 23411526]
35. Keller U, Hibst R, Geurtsen W, et al. Erbium:YAG laser application in caries therapy. Evaluation of patient perception and acceptance. J Dent 1998;26:649–56 [PubMed: 9793286]
36. Ngoc VT, Van Nga TD, Chu DT, Anh LQ. Pulpotomy management using laser diode in pediatric patient with severe hemophilia A under general anesthesia-a case report. Spec Care Dentist 2018;38:155–9. [PubMed: 29537665]
37. Walker LA, Sanders BJ, Jones JE, et al. Current trends in pulp therapy: a survey analyzing pulpotomy techniques taught in pediatric dental residency programs. J Dent Child (Chic) 2013;80:31–5. [PubMed: 23595242]
38. Dela Rosa A, Sarma AV, Le CQ, et al. Peripheral thermal and mechanical damage to dentin with microsecond and sub-microsecond 9.6 microm, 2.79 microm, and 0.355 microm laser pulses. Lasers Surg Med 2004;35:214–28. [PubMed: 15389737]
39. Fried D, Zuerlein MJ, Le CQ, Featherstone J. Thermal and chemical modification of dentin by 9-11 μm CO_2 laser pulses of 5-100-μs duration. Lasers Surg Med 2002;3:275–82.
40. Nguyen D, Chang K, Hedayatollahnajafi S, et al. High-speed scanning ablation of dental hard tissues with a λ=9.3 μm CO_2 laser: adhesion, mechanical strength, heat accumulation, and peripheral thermal damage. J Biomed Opt 2011;16:071410. [PubMed: 21806256]

SIGNIFICANCE

This study presents a laser-based dynamic navigation system designed to execute guided endodontic access for minimally invasive endodontics. This instrument has potential for *in vivo* clinical use in the future to perform the duties demonstrated in this article.

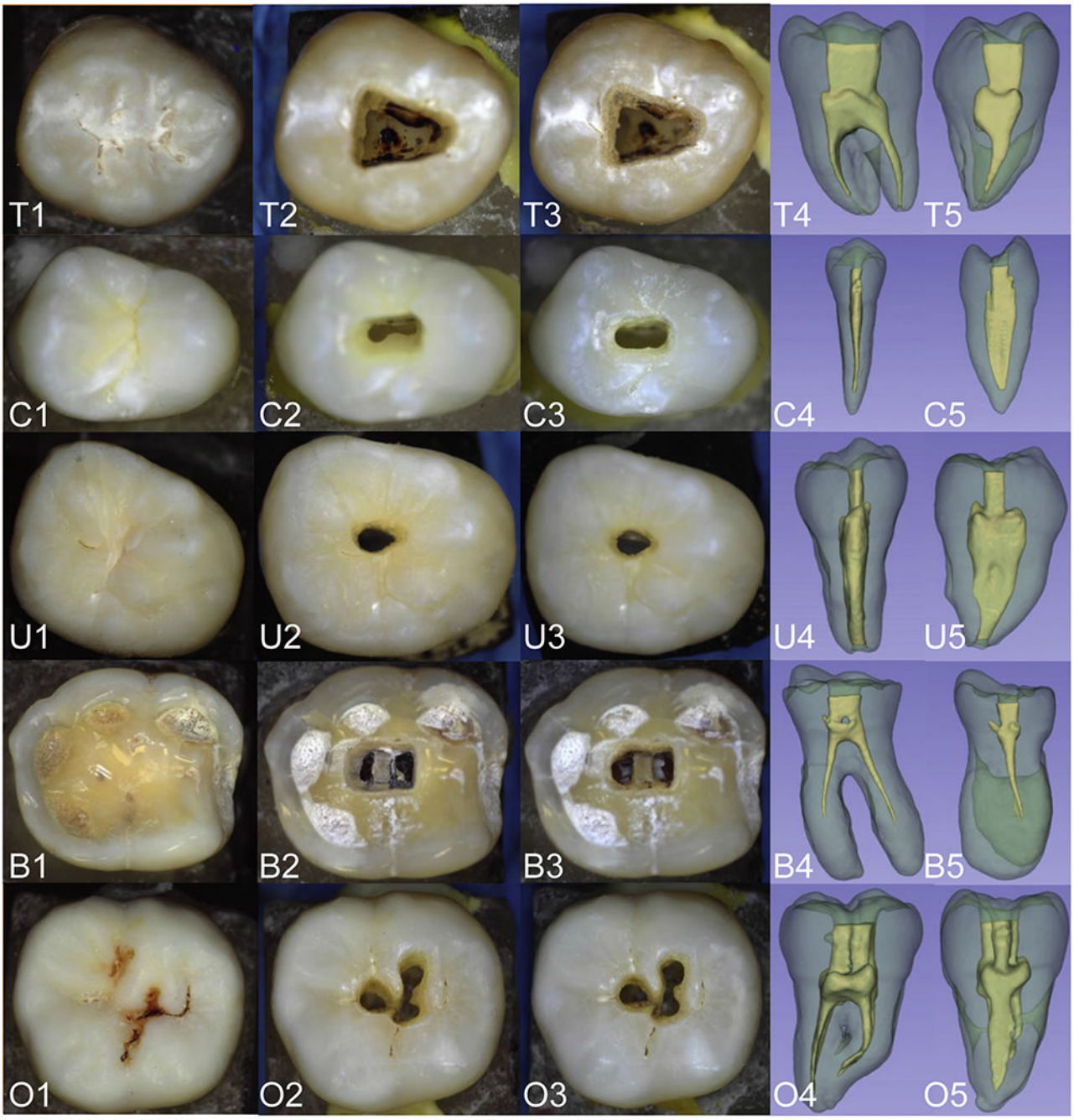

FIGURE 1 –.

(*T*) Traditional, (*C*) conservative, (*U*) ultraconservative, (*B*) bridge, and (*O*) orifice-directed (*O*) accesses cut with a CO_2 laser. Visible microscopic images showing (*1*) preablation, (*2*) post–laser access, and (*3*) post–crown-down treatments. Volumetric renderings showing (*4*) mesiodistal and (*5*) buccolingual views.

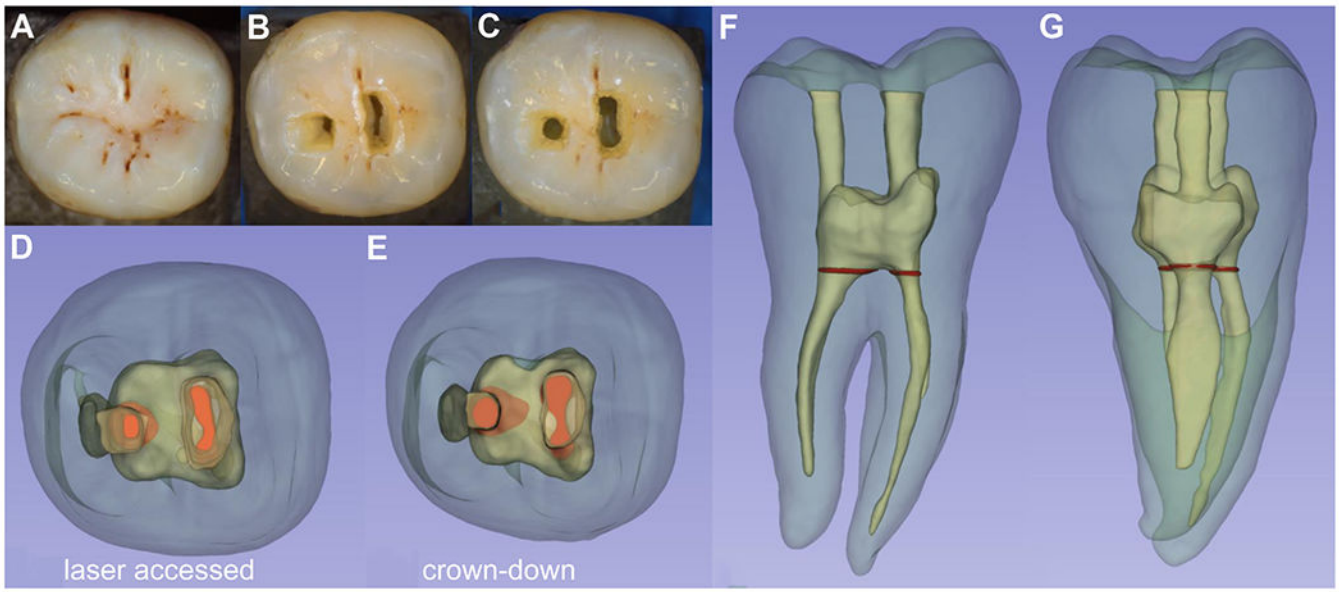

FIGURE 2 –.

A mandibular molar accessed with a truss design. Visible microscopic images showing (*A*) preablation, (*B*) post–laser access, and (*C*) post–crown-down treatment. Volumetric renderings of the sample occlusal surface indicating positioning of preparations (*yellow*) in relation to orifice location (*red*) from the occlusal viewpoint (*D*) after cutting with the CO_2 laser and (*E*) post–crown-down procedure. Volumetric renderings showing (*F*) mesiodistal and (*G*) buccolingual views.

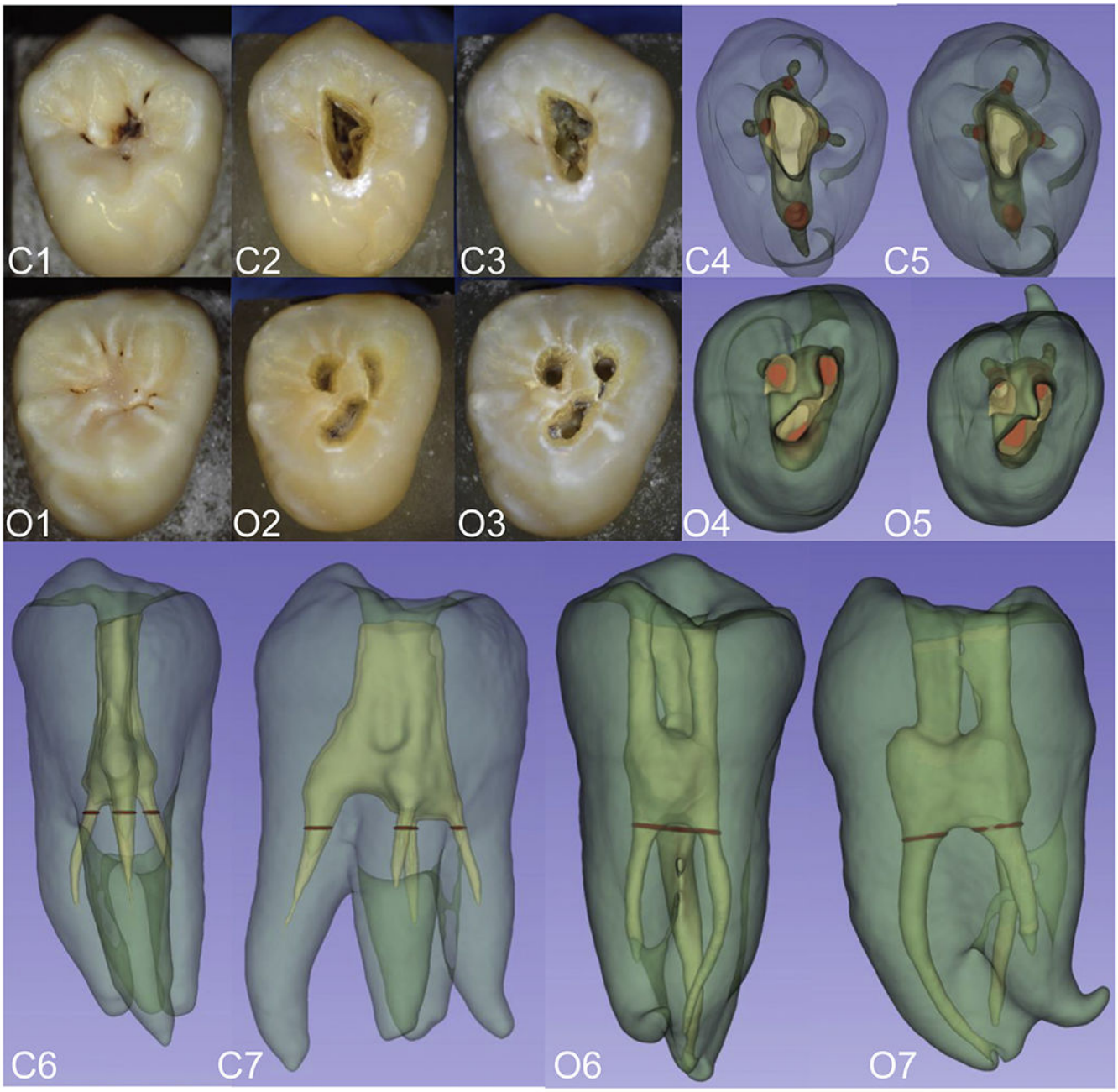

FIGURE 3 –.

Two maxillary molars prepared with a (*C*) conservative preparation and an (*O*) orifice-directed access. (*C1–C3* and *O1–O3*) Visible images (*1*) preablation, (*2*) post–laser access, and (*3*) post–crown-down treatment. Volumetric renderings showing the positioning of preparations (*yellow*) in relation to orifice location (*red*) from the occlusal viewpoint (*C4*) after cutting with the CO_2 laser and (*C5*) post–crown-down treatment. Post–crown-down renderings illustrating visualization of the (*O4*) buccal and (*O5*) palatal systems. (*C6* and

C7 and *O6* and *O7*) Volumetric renderings and demonstrate the (*6*) mesiodistal and (*7*) buccolingual views.